

Supporting Information

Pyrido[2,3-*b*]pyrazine based full-color fluorescent materials for high-performance OLEDs

Ling Yu, Zhongbin Wu, Guohua Xie, Jiajia Luo, Yang Zou, Dongge Ma and Chuluo Yang**

Corresponding Author

**E-mail: clyang@szu.edu.cn (Chuluo Yang)*

**E-mail: msdgm@scut.edu.cn (Dongge Ma)*

General Information

The ^1H NMR and ^{13}C NMR spectra were recorded on a Bruker Advance III (400 MHz) spectrometer with CDCl_3 as the solvent. Mass spectra were measured on a ZAB 3F-HF mass spectrophotometer. Matrix-assisted laser desorption ionization/time-of-flight (MALDI-TOF) mass spectra were performed on a Bruker BIFLEX III TOF mass spectrometer. Elemental analyses were performed on a Vario EL-III microanalyzer. Thermogravimetric analysis (TGA) was performed on a Netzsch STA 449C instrument. Differential scanning calorimetry (DSC) was performed on a NETZSCH DSC 200 PC unit at a heating rate of $20\text{ }^\circ\text{C min}^{-1}$ from 25 to $300\text{ }^\circ\text{C}$ under argon. The glass transition temperature (T_g) was determined from the second heating scan at a heating rate of $10\text{ }^\circ\text{C min}^{-1}$. UV-vis absorption spectra were recorded on a Shimadzu UV-2700 recording spectrophotometer. Photoluminescence (PL) spectra were recorded on a Hitachi F-4600 fluorescence spectrophotometer. Cyclic voltammetry (CV) was carried out in nitrogen-purged dichloromethane (oxidation scan) at room temperature with a CHI voltammetric analyzer. $\text{N-Bu}_4\text{PF}_6$ (0.1 M) was used as the supporting electrolyte. The conventional three-electrode configuration consists of a platinum working electrode, a platinum wire auxiliary electrode, and an Ag wire pseudoreference electrode with ferrocenium-ferrocene (Fc^+/Fc) as the internal standard. The PL lifetimes were measured by a single photon counting spectrometer from Edinburgh Instruments (FLS920) with a Picosecond Pulsed UV-LASTER (LASTER377) as the excitation source. The photoluminescence quantum efficiency was measured using an absolute photoluminescence quantum yield measurement system (C9920-02, Hamamatsu Photonics).

Devices fabrication and characterization

The device was grown on clean glass substrates pre-coated with a 180-nm-thick ITO with a sheet resistance of 10Ω per square. The ITO glass substrates were pre-cleaned carefully and treated by oxygen plasma for 2 min. Then the sample was transferred to the deposition system. 10 nm MoO_3 was firstly deposited onto the ITO substrate, consecutively followed by TAPC (50 nm), mCP (10 nm), emissive layer (20 nm), BmPyPB (10 nm) and BmPyPB: 3% Li_2CO_3 (45 nm). Finally, a cathode composed of lithium carbonate and aluminum was sequentially deposited onto the sample in the vacuum of 10^{-6} Torr. The current-voltage-brightness characteristic was measured by using a Keithley source measurement unit (Keithley 2400 and Keithley 2000) with a calibrated silicon photodiode. The EL spectra were measured by a Spectrascan PR650 spectrophotometer. The EQE was calculated from the luminance, the EL spectrum, and the current density.

Synthesis of materials

2,3-diphenyl-7-(5*H*-Iminostilbene-yl)-pyrido[2,3-*b*]pyrazine (**SBPQ-BAZ**): A mixture of SBPQ (1.20 g, 3.31 mmol), 5*H*-Iminostilbene (0.83 g, 4.30 mmol), Pd(OAc)₂ (20 mg, 0.09 mmol), HP(*t*-Bu)₃BF₄ (64 mg, 0.22 mmol), *t*-BuONa (0.52 g, 5.42 mmol), and toluene (30 mL) was refluxed under argon for 24 h. After cooled, the mixture was extracted with brine and CH₂Cl₂, and dried over anhydrous Na₂SO₄. After removal of the solvent, the residue was purified by column chromatography on silica gel using dichloromethane/petroleum ether (5:1 by vol.) as the eluent to give a yellow powder (1.20 g, yield: 76%). ¹H NMR (400 MHz, CDCl₃) δ [ppm]: 8.42 (d, *J* = 4.0 Hz, 1H), 7.61-7.56 (m, 4H), 7.52-7.49 (m, 4H), 7.47-7.40 (m, 4H), 7.33-7.28 (m, 5H), 7.25 (t, *J* = 2.0 Hz, 1H), 7.11 (d, *J* = 4.0 Hz, 1H), 6.87 (s, 2H). ¹³C NMR (100 MHz, CDCl₃) δ [ppm]: 154.72, 151.66, 145.73, 144.40, 143.85, 141.25, 139.14, 138.52, 137.13, 135.71, 130.82, 130.52, 130.14, 129.61, 129.45, 128.84, 128.64, 128.34, 128.15, 128.00, 113.18. MS (EI): *m/z* 474 [M⁺]. Elemental analysis (%) for C₃₃H₂₂N₄: C 83.52, H 4.67, N 11.81; Found: C 83.59, H 4.74, N 11.88.

2,3-diphenyl-7-(3,6-di-*tert*-butylcarbazole-9*H*-yl)-pyrido[2,3-*b*]pyrazine (**SBPQ-*t*BuCz**): A mixture of **SBPQ** (1.20 g, 3.31 mmol), 3,6-di-*tert*-butyl-9*H*-carbazole (1.47 g, 4.98 mmol), K₂CO₃ (2.28 g, 16.5 mmol), CuI (0.11 g, 0.58 mmol) and 18-crown-6 (0.15 g, 0.58 mmol) were dissolved in 1,2-dichlorobenzene (5 mL) under nitrogen atmosphere. The reaction mixture was stirred for 48 h at 180 °C. After cooled, the mixture was extracted with brine and CH₂Cl₂, and dried over anhydrous Na₂SO₄. After removal of the solvent, the residue was purified by column chromatography on silica gel using dichloromethane/petroleum ether (3:2 by vol.) as the eluent to give a yellow powder (1.82 g, yield: 98%). ¹H NMR (400 MHz, CDCl₃) δ [ppm]: 9.47 (d, *J* = 4.0 Hz, 1H), 8.71 (d, *J* = 4.0 Hz,

1H), 8.19 (s, 2H), 7.68 (t, $J = 4.0$ Hz, 2H), 7.62-7.59 (m, 2H), 7.56-7.51 (m, 4H), 7.45-7.36 (m, 6H), 1.49 (s, 18H). ^{13}C NMR (100 MHz, CDCl_3) δ [ppm]: 156.05, 155.56, 152.70, 148.02, 144.49, 138.49, 138.00, 136.50, 135.96, 130.31, 129.90, 129.56, 128.56, 128.30, 124.28, 116.73, 108.91, 34.89, 31.99. MS (EI): m/z 560 [M^+]. Elemental analysis (%) for $\text{C}_{39}\text{H}_{36}\text{N}_4$: C 83.54, H 6.47, N 9.99; Found: C 83.67, H 6.48, N 10.14.

2,3-diphenyl-7-[3,6-(3,6-di-*tert*-butylcarbazole)-carbazole-9*H*-yl]-pyrido[2,3-*b*]pyrazine (**SBPQ-DtBuCz**): it was prepared by the same procedure with **SBPQ-tBuCz** excepting using 3,6-bis(3,6-di-*tert*-butylcarbazol-9-yl)carbazole (**DtBuCz**) (2.39 g, 3.31 mmol) to replace 3,6-di-*tert*-butyl-9*H*-carbazole. **SBPQ-DtBuCz** is a yellow powder (2.5 g, yield: 90%). ^1H NMR (400 MHz, CDCl_3) δ [ppm]: 9.62 (d, $J = 4.0$ Hz, 1H), 8.91 (s, 1H), 8.31 (s, 2H), 8.17 (s, 4H), 7.81 (d, $J = 8.0$ Hz, 2H), 7.73-7.64 (m, 6H), 7.49-7.47 (m, 5H), 7.43-7.36 (m, 9H), 1.47 (s, 36H). ^{13}C NMR (100 MHz, CDCl_3) δ [ppm]: 156.88, 156.01, 152.63, 148.70, 142.80, 139.97, 139.73, 138.24, 137.85, 136.35, 134.92, 132.20, 130.37, 129.93, 128.64, 128.40, 126.55, 124.92, 123.72, 123.25, 119.66, 116.34, 110.85, 109.06, 34.80, 32.09. MS (EI): m/z 1003 [M^+]. Elemental analysis (%) for $\text{C}_{71}\text{H}_{66}\text{N}_6$: C 84.99, H 6.63, N 8.38; Found: C 84.75, H 6.63, N 8.28.

2,3-diphenyl-7-(9,9-diphenyl-9,10-dihydroacridine-10-yl)-pyrido[2,3-*b*]pyrazine (**SBPQ-DPAC**): it was prepared by the same procedure with **SBPQ-BAZ** excepting using 9,9-diphenyl-9,10-dihydroacridine (DPAC) (1.10 g, 3.31 mmol) to replace 5*H*-Iminostilbene. **SBPQ-DPAC** is a yellow powder (1.46 g, yield: 86%). ^1H NMR (400 MHz, CDCl_3) δ [ppm]: 8.59 (s, 1H), 8.42 (d, $J = 4.0$ Hz, 1H), 7.65 (t, $J = 4.0$ Hz, 2H), 7.57 (t, $J = 4.0$ Hz, 2H), 7.44-7.27 (m, 12H), 7.13-7.09 (m, 2H), 7.01-

6.98 (m, 8H), 6.61 (d, $J = 8.0$ Hz, 2H). ^{13}C NMR (100 MHz, CDCl_3) δ [ppm]: 156.72, 156.35, 155.13, 148.57, 146.67, 141.56, 138.44, 138.32, 138.14, 137.91, 136.39, 131.93, 130.50, 130.38, 129.82, 129.55, 128.54, 128.28, 127.85, 127.18, 126.65, 121.61, 115.08. MS (EI): m/z 625 [M^+]. Elemental analysis (%) for $\text{C}_{44}\text{H}_{30}\text{N}_4$: C 85.97, H 4.92, N 9.11; Found: C 85.90, H 4.93, N 9.15.

2,3-diphenyl-7-(9,9-dimethyl-9,10-dihydroacridine-10-yl)-pyrido[2,3-*b*]pyrazine (**SBPQ-DMAC**): it was prepared by the same procedure with **SBPQ-BAZ** excepting using 9,9-dimethyl-9,10-dihydroacridine (DMAC) (0.90 g, 4.30 mmol) to replace 5*H*-Iminostilbene. **SBPQ-DMAC** is an orange powder (1.50 g, yield: 92%). ^1H NMR (400 MHz, CDCl_3) δ [ppm]: 9.11 (s, 1H), 8.62 (s, 1H), 7.79 (d, $J = 8.0$ Hz, 2H), 7.60 (d, $J = 8.0$ Hz, 2H), 7.53 (t, $J = 4.0$ Hz, 2H), 7.45-7.35 (m, 6H), 7.05-7.01 (m, 4H), 6.44 (t, $J = 4.0$ Hz, 2H), 1.74 (s, 6H). ^{13}C NMR (100 MHz, CDCl_3) δ [ppm]: 157.05, 156.54, 155.19, 148.75, 140.35, 139.02, 138.75, 138.29, 137.95, 136.72, 130.30, 129.88, 128.53, 128.31, 126.66, 125.54, 121.99, 114.73, 36.27, 30.99, 30.73. MS (EI): m/z 490 [M^+]. Elemental analysis (%) for $\text{C}_{34}\text{H}_{26}\text{N}_4$: C 83.24, H 5.34, N 11.42; Found: C 83.45, H 5.40, N 11.40.

2,3-diphenyl-7-(10*H*-phenoxazin-10-yl)-pyrido[2,3-*b*]pyrazine (**SBPQ-PXZ**): it was prepared by the same procedure with **SBPQ-BAZ** excepting using 10*H*-phenoxazin (PXZ) (0.79 g, 4.31 mmol) to replace 5*H*-Iminostilbene. **SBPQ-PXZ** is a red powder (1.50 g, yield: 97%). ^1H NMR (400 MHz, CDCl_3) δ [ppm]: 9.14 (s, 1H), 8.60 (s, 1H), 7.67 (d, $J = 8.0$ Hz, 2H), 7.59 (d, $J = 8.0$ Hz, 2H), 7.44-7.35 (m, 6H), 6.82-6.74 (m, 4H), 6.65 (t, $J = 8.0$ Hz, 2H), 6.11 (d, $J = 8.0$ Hz, 2H). ^{13}C NMR (100 MHz, CDCl_3) δ [ppm]: 156.88, 155.28, 148.90, 144.23, 139.81, 138.17, 137.82, 136.61, 136.48, 133.19, 130.29, 129.86, 129.67, 128.55, 128.33, 123.50, 122.74, 116.20, 113.52. MS (EI): m/z 464

[M⁺]. Elemental analysis (%) for C₃₁H₂₀N₄O: C 80.15, H 4.34, N 12.06; Found: C 80.25, H 4.48, N 12.00.

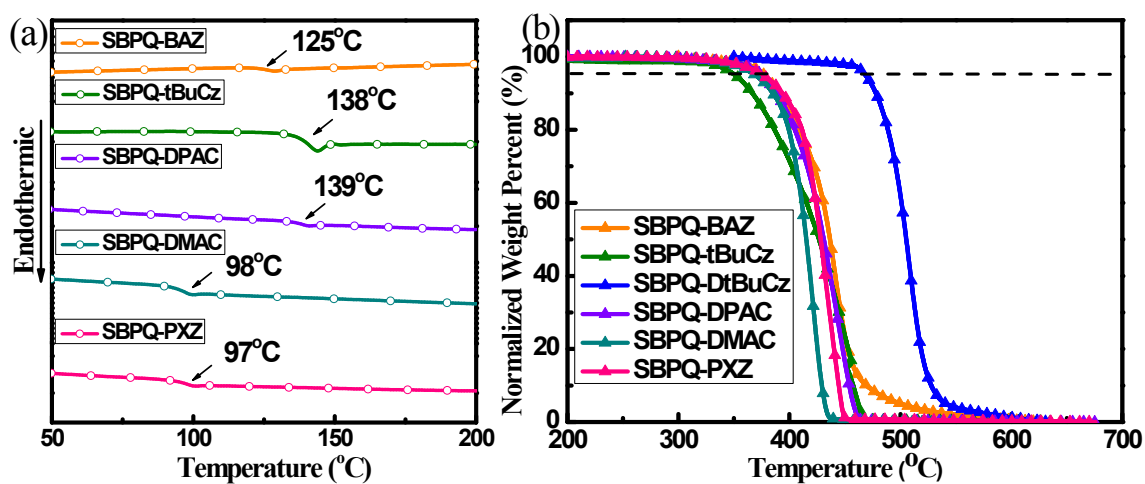


Figure S1. (a) Differential scanning calorimetry (DSC) curves and (b) thermal gravity analysis (TGA) curves of the target compounds.

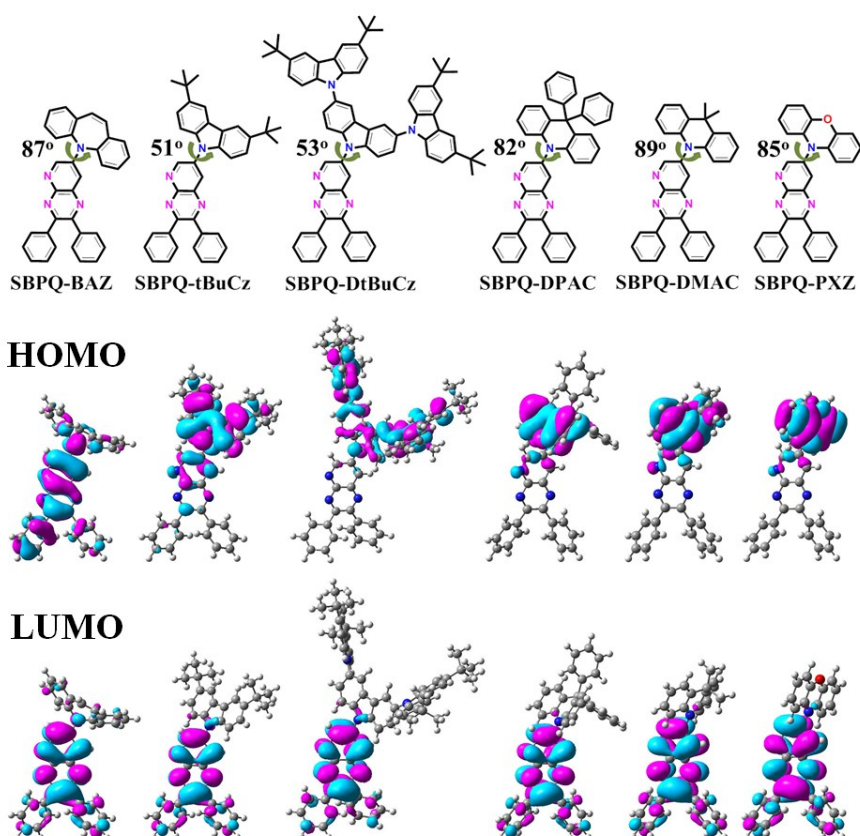


Figure S2. Molecular structures (upper), and the HOMO/LUMO distributions evaluated by using b3lyp/6-31g(d) level.

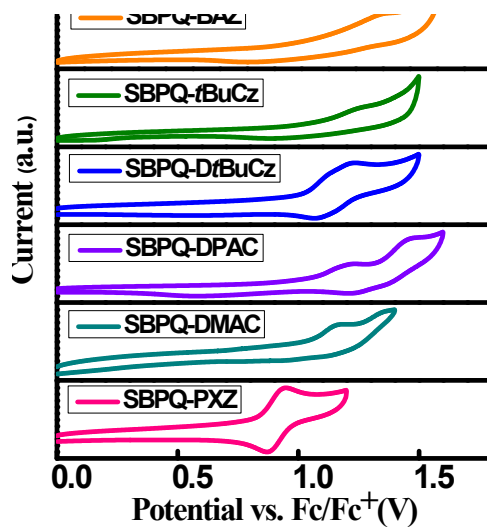


Figure S3. Cyclic voltammogram of target compounds in CH_2Cl_2 for oxidation scan.

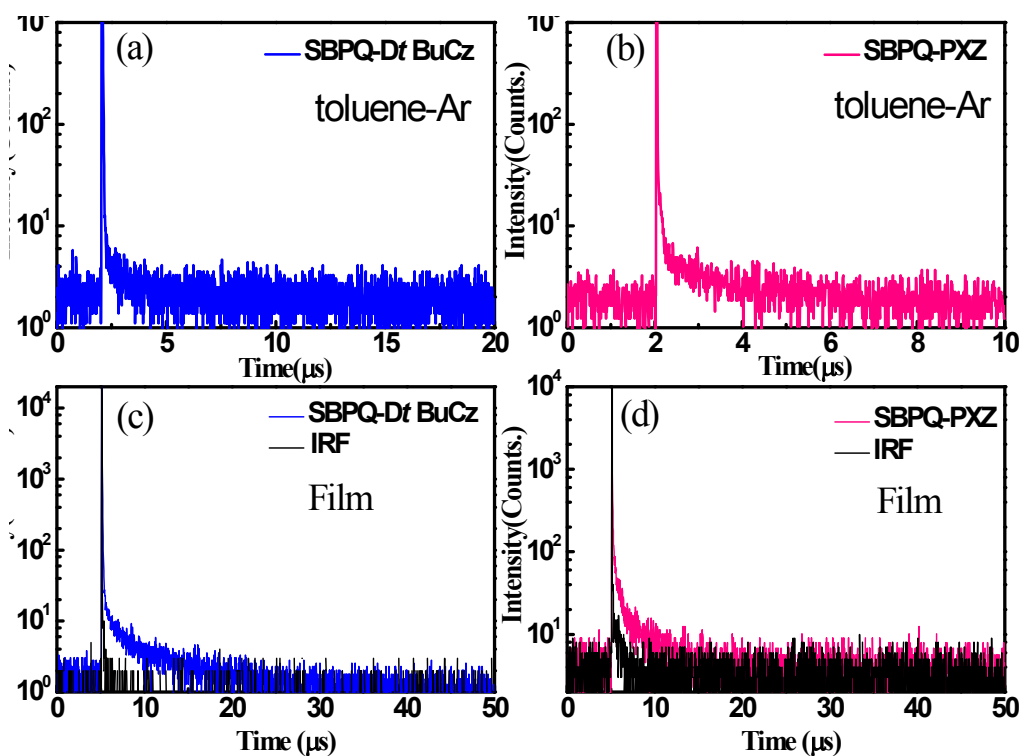


Figure S4. Transient PL characteristics of SBPQ-DtBuCz and SBPQ-PXZ (a-b) in toluene (10^{-4} M) under argon conditions and (c-d) in film at room temperature.

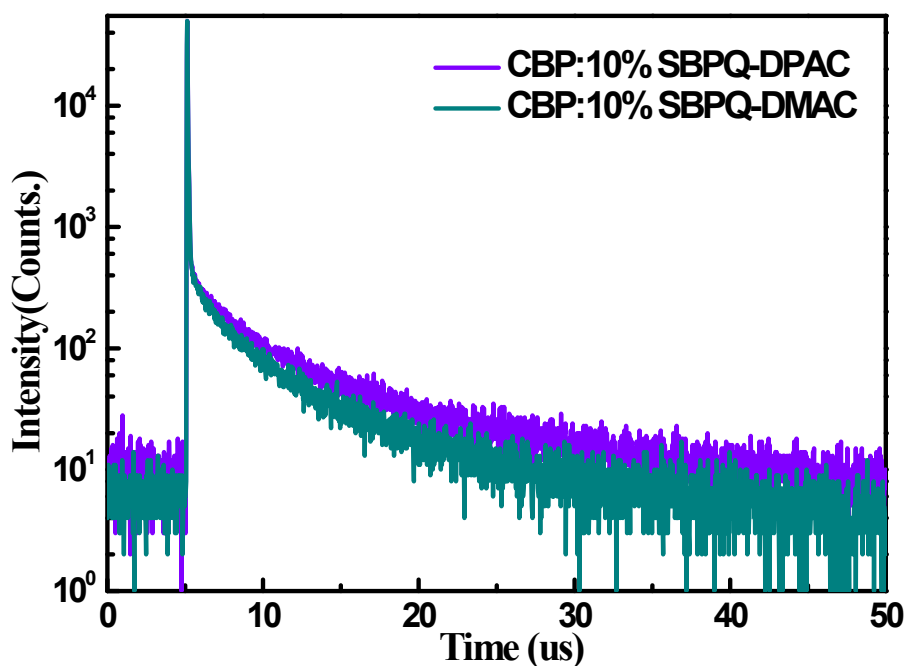


Figure S5. Transient PL decay of CBP:10% TADF in films after the deoxygenation at room temperature.

Table S1. The lifetimes, quantum efficiencies and rate constants of CBP: 10% TADF in film.

TADF Compounds	τ_F [ns]	τ_d [μ s]	$\Phi_{PL}^{[a]}$ [%]	$\Phi_{DF}^{[a]}$ [%]	$k_p^{[b]}$ [s^{-1}]	$k_d^{[b]}$ [s^{-1}]	$k_r^{S[c]}$ [s^{-1}]	$k_{ISC}^{[d]}$ [s^{-1}]	$k_{RISC}^{[d]}$ [s^{-1}]
SBPQ-DPAC	37	4.8	98	43	2.7×10^7	2.1×10^5	1.5×10^7	1.2×10^7	3.7×10^5
SBPQ-DMAC	38	4.0	61	24	2.6×10^7	2.5×10^5	9.6×10^6	1.6×10^7	2.6×10^5

^[a]The total and delayed fluorescence quantum yield, respectively. ^[b]The rate constant for prompt and delayed fluorescence, respectively. ^[c] k_r^S represents the radiative decay rate constant from S_1 to S_0 transition. ^[d]The rate constants for intersystem crossing (ISC) and reverse intersystem crossing (RISC) between the S_1 and T_1 states, respectively.

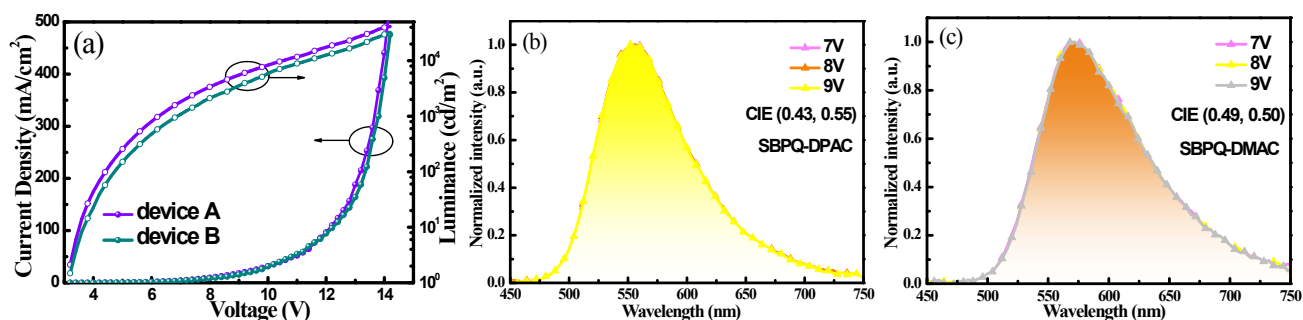


Figure S6. (a) current density-voltage-brightness characteristics, (b-c) EL spectra of the doped devices (A and B) measured at different voltages, respectively.

Table S2. Comparison of the device data for the representative yellow and orange/red TADF-OLEDs.

Device	$V_{on}^{[a]}$ [V]	EQE_{max} [%]	CE_{max} [cd A ⁻¹]	PE_{max} [lm W ⁻¹]	LE_{max} [cd m ⁻²]	Peak ^[b] [nm]	Reference
Spiro-CN	~3.0	4.4	13.5	13.0	12000	~545	Chem. Commun. 2012 , 48, 9580. ^[S1]
TXO-TPA	5.3	18.5	43.3	47.4	16300	552	Adv. Mater. 2014 , 26, 5198. ^[S2]
PxPmBPX	3.2	11.3	35.3	N.A.	61040	541	Dalton Trans. 2015 , 44, 8356. ^[S3]
TPA-PRZ(CN) ₂	N.A.	4.0	N.A.	N.A.	N.A.	542	J.Am.Chem.Soc. 2015 , 137, 11908. ^[S4]
Bis-PXZTRZ	N.A.	9.1	N.A.	N.A.	N.A.	~552	Chem. Mater. 2013 , 25, 3766. ^[S5]
PXZDSO ₂	3.7	16.7	49.3	38.5	17000	560	Adv. Mater. 2016 , 28, 181. ^[S6]
Py56	~2.5	29.2	96.3	105.5	N.A.	~550	Adv. Funct. Mater. 2016 , 26, 7560. ^[S7]
DBT-BZ-PXZ	2.9	9.2	26.6	27.9	N.A.	557	Chem. Mater. 2017 , 29, 3623. ^[S8]
DBT-BZ-PTZ	2.7	9.7	26.5	29.1	N.A.	563	
Ac-CNP	4.7	13.3	38.1	26.1	70630	580	Adv.Funct.Mater. 2016 , 26, 1813. ^[S9]
HAP-3TPA	4.4	17.5	25.9	22.1	17000	~600	Adv. Mater. 2013 , 25, 3319. ^[S10]
Ac-CNBQx	2.8	14.0	34.0	33.3	N.A.	585	Adv. Optical Mater. 2018 , 6, 1701147. ^[S11]
3	N.A.	17.5	55.7	58.4	N.A.	544	Angew. Chem. Int. Ed. 2019 , 58, 9088. ^[S12]
SBPQ-DPAC	3.2	20.0	65.7	59.0	41350	556	This work
SBPQ-DMAC	3.2	15.4	41.5	40.7	32505	572	This work

^[a]At a luminance of 1 cd m⁻²; ^[b]The peak wavelength of EL spectrum. N.A.: not available.

References

- [S1] T. Nakagawa, S. Y. Ku, K. T. Wong and C. Adachi, *Chem. Commun.*, 2012, **48**, 9580-9582.
- [S2] H. Wang, L. Xie, Q. Peng, L. Meng, Y. Wang, Y. Yi and P. Wang, *Adv. Mater.*, 2014, **26**, 5198-5204.
- [S3] S. Y. Lee, T. Yasuda, I. S. Park and C. Adachi, *Dalton Trans.*, 2015, **44**, 8356-8359.
- [S4] K. Kawasumi, T. Wu, T. Zhu, H. S. Chae, T. Van Voorhis, M. A. Baldo and T. M. Swager, *J. Am. Chem. Soc.*, 2015, **137**, 11908-11911.
- [S5] H. Tanaka, K. Shizu, H. Nakanotani and C. Adachi, *Chem. Mater.*, 2013, **25**, 3766-3771.
- [S6] G. Xie, X. Li, D. Chen, Z. Wang, X. Cai, D. Chen, Y. Li, K. Liu, Y. Cao and S. J. Su, *Adv. Mater.*, 2016, **28**, 181-187.
- [S7] K.-C. Pan, S.-W. Li, Y.-Y. Ho, Y.-J. Shiu, W.-L. Tsai, M. Jiao, W.-K. Lee, C.-C. Wu, C.-L. Chung, T. Chatterjee, Y.-S. Li, K.-T. Wong, H.-C. Hu, C.-C. Chen and M.-T. Lee, *Adv. Funct. Mater.*, 2016, **26**, 7560-7571.
- [S8] J. Guo, X.-L. Li, H. Nie, W. Luo, R. Hu, A. Qin, Z. Zhao, S.-J. Su and B. Z. Tang, *Chem. Mater.*, 2017, **29**, 3623-3631.
- [S9] I. S. Park, S. Y. Lee, C. Adachi and T. Yasuda, *Adv. Funct. Mater.*, 2016, **26**, 1813-1821.
- [S10] J. Li, T. Nakagawa, J. MacDonald, Q. Zhang, H. Nomura, H. Miyazaki and C. Adachi, *Adv. Mater.*, 2013, **25**, 3319-3323.
- [S11] R. Furue, K. Matsuo, Y. Ashikari, H. Ooka, N. Amanokura and T. Yasuda, *Adv. Optical Mater.*, 2018, **6**, 1701147.
- [S12] P. Li, H. Chan, S. L. Lai, M. Ng, M. Y. Chan and V. W. Yam, *Angew. Chem. Int. Ed.*, 2019, **58**, 9088-9094.